

Article

**Purified Anthocyanins from Bilberry and Black Currant  
Attenuate Hepatic Mitochondrial Dysfunction and  
Steatohepatitis in Mice with Methionine and Choline Deficiency**

Honghui Guo

*J. Agric. Food Chem.*, **Just Accepted Manuscript** • DOI: 10.1021/jf504926n • Publication Date (Web): 23 Dec 2014

Downloaded from <http://pubs.acs.org> on December 27, 2014

**Just Accepted**

“Just Accepted” manuscripts have been peer-reviewed and accepted for publication. They are posted online prior to technical editing, formatting for publication and author proofing. The American Chemical Society provides “Just Accepted” as a free service to the research community to expedite the dissemination of scientific material as soon as possible after acceptance. “Just Accepted” manuscripts appear in full in PDF format accompanied by an HTML abstract. “Just Accepted” manuscripts have been fully peer reviewed, but should not be considered the official version of record. They are accessible to all readers and citable by the Digital Object Identifier (DOI®). “Just Accepted” is an optional service offered to authors. Therefore, the “Just Accepted” Web site may not include all articles that will be published in the journal. After a manuscript is technically edited and formatted, it will be removed from the “Just Accepted” Web site and published as an ASAP article. Note that technical editing may introduce minor changes to the manuscript text and/or graphics which could affect content, and all legal disclaimers and ethical guidelines that apply to the journal pertain. ACS cannot be held responsible for errors or consequences arising from the use of information contained in these “Just Accepted” manuscripts.



**ACS Publications**  
High quality. High impact.

Journal of Agricultural and Food Chemistry is published by the American Chemical Society, 1155 Sixteenth Street N.W., Washington, DC 20036  
Published by American Chemical Society. Copyright © American Chemical Society.  
However, no copyright claim is made to original U.S. Government works, or works produced by employees of any Commonwealth realm Crown government in the course of their duties.

This document is confidential and is proprietary to the American Chemical Society and its authors. Do not copy or disclose without written permission. If you have received this item in error, notify the sender and delete all copies.

**Purified Anthocyanins from Bilberry and Black Currant  
Attenuate Hepatic Mitochondrial Dysfunction and  
Steatohepatitis in Mice with Methionine and Choline  
Deficiency**

Journal:	<i>Journal of Agricultural and Food Chemistry</i>
Manuscript ID:	jf-2014-04926n.R1
Manuscript Type:	Article
Date Submitted by the Author:	08-Dec-2014
Complete List of Authors:	Tang, Xilan; Department of Nutrition, School of Public Health, Sun Yat-Sen University, Shen, Tianran; Department of Nutrition, School of Public Health, Sun Yat-Sen University, Jiang, Xinwei; Department of Nutrition, School of Public Health, Sun Yat-Sen University, Xia, Min; Department of Nutrition, School of Public Health, Sun Yat-Sen University, ; Guangdong Provincial Key Laboratory of Food, Nutrition and Health, Sun, Xujia; Department of Nutrition, School of Public Health, Sun Yat-Sen University, Guo, Honghui; Shaoguan University, Department of Nutrition Ling, Wenhua; Department of Nutrition, School of Public Health, Sun Yat-Sen University, ; Guangdong Provincial Key Laboratory of Food, Nutrition and Health,

SCHOLARONE™  
Manuscripts

**Purified Anthocyanins from Bilberry and Black Currant Attenuate Hepatic  
Mitochondrial Dysfunction and Steatohepatitis in Mice with Methionine and  
Choline Deficiency**

Xilan Tang,<sup>†</sup> Tianran Shen,<sup>†</sup> Xinwei Jiang,<sup>†</sup> Min Xia,<sup>†,‡</sup> Xujia Sun,<sup>†</sup> Honghui Guo,<sup>\*,§</sup>  
and Wenhua Ling<sup>\*,†,‡</sup>

<sup>†</sup>Department of Nutrition, School of Public Health, Sun Yat-Sen University,  
Guangzhou, P. R. China

<sup>§</sup>Department of Nutrition, Henry Fok School of Food Science and Engineering,  
Shaoguan University, Shaoguan 512005, P. R. China

<sup>‡</sup>Guangdong Provincial Key Laboratory of Food, Nutrition and Health, Guangzhou, P.  
R. China

\*Correspondence:

Dr. Honghui Guo, Department of Nutrition, Henry Fok School of Food Science and  
Engineering, Shaoguan University, Shaoguan 512005, P. R. China

E-mail: [guohh1999@hotmail.com](mailto:guohh1999@hotmail.com)

Tel.: 86-751-8120167

Fax: 86-751-8121429;

Dr. Wenhua Ling, Department of Nutrition, School of Public Health, Sun Yat-Sen  
University, Guangzhou, 510080, P. R. China

E-mail: [lingwh@mail.sysu.edu.cn](mailto:lingwh@mail.sysu.edu.cn)

Tel.: 86-20-87331597

Fax: 86-20-87330446

## ABSTRACT

The berries of bilberry and black currant are rich source of anthocyanins, which are thought to have favorable effects on non-alcoholic steatohepatitis (NASH). This study was designed to examine whether purified anthocyanins from bilberry and black currant are able to limit the disorders related to NASH induced by a methionine-choline-deficient (MCD) diet in mice. The results showed that treatment with anthocyanins not only alleviated inflammation, oxidative stress, steatosis and even fibrosis, but also improved the depletion of mitochondrial content and damage of mitochondrial biogenesis and electron transfer chain developed concomitantly in the liver of mice fed the MCD diet. Furthermore, anthocyanins treatment promoted activation of AMP-activated protein kinase (AMPK) and expression of peroxisome proliferator-activated receptor-gamma coactivator-1 $\alpha$  (PGC-1 $\alpha$ ). These data provide evidence that anthocyanins possess significant protective effects against NASH and mitochondrial defects in response to a MCD diet, with mechanism maybe through affecting the AMPK/PGC-1 $\alpha$  signaling pathways.

**KEYWORDS:** *AMP-activated protein kinase; anthocyanin; mitochondrial dysfunction; nonalcoholic fatty liver disease; oxidative stress*

## INTRODUCTION

Non-alcoholic fatty liver disease (NAFLD) is currently the most prevalent chronic liver disease, largely due to obesity epidemic.<sup>1</sup> It encompasses a spectrum of liver damage ranging from simple steatosis to non-alcoholic steatohepatitis (NASH), an advanced stage of disease comprising progressive steatosis, lobular inflammation, balloon degeneration and even fibrosis.<sup>2</sup> The pathogenesis responsible for the development and progression of NASH is comprehensive and remains yet to be fully elucidated. Due to this, available treatments remain unsatisfactory.

Hepatocytes are commonly enriched in mitochondria (~1000-2000 mitochondria/hepatocyte), signifying their critical roles within hepatocytes, such as the primary site for energy production and  $\beta$ -oxidation of fatty acids. Previous studies have shown that abnormal morphological changes in mitochondria and reduced mitochondrial DNA (mtDNA) copy number are observed in human subjects and animal models with NASH.<sup>3,4</sup> In addition, significantly decreased activity of the hepatic mitochondrial respiratory chain (MRC), particularly complex I and IV, was shown in NASH liver samples compared to controls.<sup>5,6</sup> Moreover, recent evidence has demonstrated impairment of mitochondrial  $\beta$ -oxidation in humans and animals with NASH.<sup>7,8</sup> These studies provide strong evidence to support the possibility that NAFLD might be a mitochondrial disease. They also support seeking therapies that improve mitochondrial function as a useful strategy for preventing NASH and its complications.

Interestingly, several polyphenolic compounds, such as curcumin,<sup>9</sup> quercetin,<sup>10</sup>

anthocyanins (ACNs)<sup>11</sup> and green tea catechins<sup>12</sup>, have been demonstrated to have beneficial effects in NAFLD. Among them, ACNs are of great interest due to their abundance in a wide variety of plant foods and the fact that considerable amounts could be ingested from our plant-based daily diets. Existing *in vitro* data suggest that ACNs exert anti-steatosis effects in hepatocytes by inhibiting lipogenesis and/or promoting fatty acid oxidation.<sup>13-15</sup> Mirroring the results obtained *in vitro*, ample evidence from animal models of NAFLD demonstrates that ACNs diminish hepatic lipid accumulation and inflammation.<sup>16</sup> Furthermore, ACNs are thought to promote antioxidant activity and eventually contribute to an overall positive gain in liver function.<sup>17,18</sup> Despite realizing these benefits, an understanding of the protective role of ACNs and the underlying mechanism of action in the progression of NASH remains unknown and requires further investigation *in vivo*.

Considering the potential capability of ACNs in NASH and the vital role of mitochondrial dysfunction in the progression of NASH, we set out to determine the influence of purified ACNs from bilberry and black currant on hepatic steatohepatitis and fibrosis as well as mitochondrial content and function in a methionine-choline-deficient (MCD) diet murine model of NASH. The influence of ACNs on related signaling pathways was also investigated.

## MATERIALS AND METHODS

**Purified Anthocyanins.** Purified ACNs were kindly provided by Polyphenol AS (Sandnes, Norway). As mentioned in our previous study,<sup>19</sup> the purified ACNs product is consisted of 17 different natural ACNs from bilberry (*Vaccinium myrtillus*) and

63 black currant (*Ribes nigrum*). Cyanidin 3-*O*- $\beta$ -glucoside and delphinidin  
64 3-*O*- $\beta$ -glucoside are major components of the ACNs supplement. Detailed  
65 components and contents are listed in Supporting Information Table 1.

66 **Reagents and Antibodies.** Reagents for immunohistochemistry and  
67 immunofluorescence, such as serum blocking solution, hydrogen peroxide and  
68 diaminobenzidine (DAB), were obtained from Zhongshan Jinqiao Biotechnology Co  
69 (Beijing, China). Anti-AMP-activated protein kinase (AMPK) and  
70 anti-phosphorylated AMP-activated protein kinase (p-AMPK) antibodies were  
71 purchased from Cell Signaling Technology Inc. (Danvers, MA, USA). Antibodies for  
72 cabamoyl phosphate synthase 1 (CPS-1), alpha smooth muscle actin ( $\alpha$ -SMA),  
73 peroxisome proliferator-activated receptor- $\gamma$  coactivator-1 $\beta$  (PGC-1 $\beta$ ),  
74 nicotinamide adenine dinucleotide dehydrogenase (Complex I), and cytochrome c  
75 oxidase (Complex IV) were purchased from Abcam (Cambridge, UK). Antibodies for  
76 peroxisome proliferator-activated receptor- $\gamma$  coactivator-1 $\alpha$  (PPAR- $\alpha$ ),  
77 peroxisome proliferator-activated receptor-1 $\alpha$  (PGC-1 $\alpha$ ), glyceraldehyde 3-phosphate  
78 dehydrogenase (GAPDH) and all secondary antibodies were obtained from Santa  
79 Cruz Biotechnology (Santa Cruz, CA, USA). Fluorescent probe dihydroethidium  
80 (DHE) was purchased from Calbiochem (San Diego, CA, USA). All other reagents  
81 and kits were obtained from Sigma-Aldrich (St. Louis, MO, USA) and Invitrogen  
82 (Carlsbad, CA, USA) unless otherwise noted.

83 **Animals and Diets.** All animal procedures were approved by the Animal Care and  
84 Protection Committee of Sun Yat-Sen University (2013-10). Six-week-old male

85 C57BL/6J mice purchased from the Experimental Animal Center of Sun Yat-Sen  
86 University (Guangzhou, China), were housed in standard cages within a room with a  
87 constant temperature and humidity, under a 12-h light/dark cycle, with free access to  
88 food and water. After two-week adaptation, all mice were body-weight matched and  
89 randomly divided into three groups (n = 8 per group): (1) control group, mice were  
90 fed a control chow diet; (2) MCD group, mice were fed with a diet deficient in  
91 methionine and choline; (3) MCD + ACNs group, mice were fed with the MCD diet  
92 with addition of 1 g purified ACNs per kilogram food. Both the control chow diet  
93 and MCD diet were purchased from Research Diets Inc. (New Brunswick, NJ, USA).  
94 The control diet was identical to the MCD diet but supplemented with DL-methionine  
95 (3 g/kg) and choline chloride (2 g/kg). Food intake was measured every other day and  
96 body weight was measured weekly.

97 **Biochemical Analyses.** At the end of the experiment, all mice were euthanized  
98 with sodium pentobarbital (50 mg/kg body weight) and sacrificed after overnight  
99 starvation. The serum and liver samples of each mouse were collected and stored at  
100 -80°C for further analysis.

101 Serum alanine aminotransferase (ALT) and aspartate aminotransferase (AST) were  
102 detected using commercial kits from Jiancheng Bioengineering Institute (Nanjing,  
103 China) according to the manufacturer's instructions. Serum triglyceride (TG), total  
104 cholesterol (TC), and hepatic TG/TC contents were determined using commercial  
105 detection kits (Applygen Technologies Inc., Beijing, China) according to  
106 manufacturer's protocols.



**Histological Assessment.** The liver samples were fixed in 10% phosphate-buffered formalin, embedded in paraffin, cut in 5  $\mu\text{m}$  thickness, and applied to slides. The sections were stained with hematoxylin and eosin (H&E) and Sirius Red for histological analysis (NAFLD activity scoring (NAS) and collagen) under light microscopy (Leica, Bensheim, Germany). The Pathology Committee of the NASH Clinical Research Network<sup>20</sup> provided guidance and recommendations for the NAS study by semi-quantitatively evaluating the following histological features: steatosis ( $< 5\% = 0$ ;  $5\text{--}33\% = 1$ ;  $33\text{--}66\% = 2$ ;  $>66\% = 3$ ); lobular inflammation (none = 0;  $< 2$  foci = 1;  $2\text{--}4$  foci = 2;  $>4$  foci = 3); and hepatocellular ballooning (none = 0; few = 1; prominent = 2). All features were scored blindly based on at least 5 samples per group and 10 fields of vision in each sample. Fresh liver tissue were embedded in Tissue Tek OCT and rapidly frozen in liquid nitrogen and then stored at  $-80^{\circ}\text{C}$  for preparation of frozen sections (5  $\mu\text{m}$ ), which were used for staining with Oil Red O and immunofluorescence staining.

**Immunohistochemistry and Immunofluorescence.** The procedures for immunohistochemistry and immunofluorescence assays were performed as previously described.<sup>21</sup> Briefly, slides were incubated in serum blocking solution for 30 min and incubated overnight with either  $\alpha$ -SMA or CPS-1 primary antibody. Then HRP-labeled or fluorescent secondary antibodies were used for immunohistochemistry ( $\alpha$ -SMA) and immunofluorescence (CPS-1) analysis, respectively. DAB was applied for immunohistochemistry and the samples were observed under light microscopy (Leica, Bensheim, Germany). DAPI (Roche,

Germany) was utilized for immunofluorescence nuclear staining and the samples were observed under an Inverted Fluorescence Microscopy (Nikon Eclipse Ti-E, Tokyo, Japan). The fluorescent intensity was analyzed using ImageJ software (Research Services Branch of the NIH, Bethesda, MD).

**Western Blot.** Liver tissues were homogenized and 30  $\mu$ g of total protein lysate were loaded onto 8%~15% SDS polyacrylamide gels. After 90 min of electrophoresis, the proteins were transferred onto a polyvinylidene difluoride membrane in ice for 1~2 h. The membrane was blocked with 5% (w/v) bovine serum albumin dissolved in trihydroxymethyl aminomethane buffer salt containing 0.05% (v/v) Tween-20 (TBST). The membrane was then incubated at 4°C overnight with primary antibodies for AMPK, p-AMPK, CPS-1, PGC-1 $\alpha$ , PGC-1 $\beta$ , PPAR- $\alpha$ , Complex I or Complex IV, followed by incubation with secondary antibodies conjugated with horseradish peroxidase for 2 h at room temperature. Signals were detected by enhanced chemiluminescence reagent (Thermo Fisher Scientific, Waltham, MA, USA). GAPDH was used for normalization. The density of the specific bands was quantified using ImageJ software.

**Mitochondrial DNA Quantification.** Total DNA was extracted from livers using a DNeasy Blood & Tissue Kit (Qiagen, Dusseldorf, Germany) and real-time PCR was performed using gene-specific primers amplifying mitochondrial DNA (mtDNA) and nuclear DNA (nDNA). The relative values of mtDNA content and nDNA content were used to assess mitochondrial copy numbers. The primer sequences are listed in Supporting Information Table 2.

151     **RNA Extraction and Quantitative RT-PCR.** Total RNA (1µg) was extracted from  
152     liver tissues using Trizol reagent and transcribed into cDNA using the PrimeScript RT  
153     reagent kit (TaKaRa, Tokyo, Japan) according to the manufacturer's recommendations.  
154     Quantitative PCR was performed using a real-time PCR system (Applied Biosystems,  
155     Foster City, CA, USA), and reactions were performed using SYBR Green Master Mix  
156     (TaKaRa, Tokyo, Japan) with gene-specific primers. Each sample was normalized to  
157     β-actin and the fold change in expression of each target gene relative to β-actin was  
158     assessed via the comparative CT ( $2^{-\Delta\Delta CT}$ ) method. Primer sequences are listed in  
159     Supporting Information Table 3.

160     **Detection of Hepatic Oxidative Stress.** The total reactive oxygen species (ROS)  
161     levels in the liver tissues were detected using the fluorescent probe DHE. Briefly,  
162     frozen liver sections were incubated in DHE (10 µM) for 30 min in a dark and  
163     humidified chamber at 37°C. DHE is oxidized by superoxide to ethidium bromide,  
164     bands to the DNA and emits red fluorescence,<sup>22</sup> which was detected using an Inverted  
165     Fluorescence Microscopy. In addition, liver tissue homogenates were prepared to  
166     measure hepatic malondialdehyde (MDA) by following the commercial kit's  
167     instructions (Beyotime, Shanghai, China). The MDA concentrations were normalized  
168     by protein contents.

169     **Statistical Analysis.** All results were expressed as mean ± standard deviation (SD)  
170     and statistically analyzed with SPSS 16.0 for Windows (SPSS Inc., Chicago, IL,  
171     USA). Comparisons between all groups were evaluated using one-way analysis of  
172     variance (ANOVA). Differences were considered significant at  $P < 0.05$ .

## 173 RESULTS

174 **Effects of ACNs on Animal Characteristics.** As shown in Table 1, the initial body  
175 weight amongst the 3 groups showed little deviation ( $P > 0.05$ ). After 4 weeks, the  
176 MCD mice with or without ACNs treatment displayed a significant reduction in body  
177 weight ( $\sim 50\%$ ). Moreover, one-fold increase in serum AST and more than ten-fold  
178 increase in serum ALT were observed in mice fed the MCD diet. Though ACNs didn't  
179 attenuate the reduction of body weight induced by the MCD diet, their addition  
180 effectively decreased serum ALT and AST levels ( $P < 0.05$ ). No significant changes in  
181 daily food intake among the 3 groups during the experimental period were observed  
182 (data not shown).

183 **Effects of ACNs on Lipid Accumulation.** The histological features of Oil Red O  
184 staining illustrated a massive accumulation of neutral lipid droplets within the  
185 hepatocytes of MCD group, whereas only small lipid droplets were observed in mice  
186 treated with ACNs (Figure 1A). Quantitative determination of hepatic TG content  
187 further confirmed that a large quantity of TG accumulated in the livers of mice fed the  
188 MCD diet, which was significantly decreased by ACNs supplementation ( $P < 0.05$ )  
189 (Figure 1B). Conversely, the serum TG levels in both MCD diet group and MCD +  
190 ACNs group declined sharply compared with the control group, while were slightly  
191 up-regulated by ACNs though without significance compared with the MCD group  
192 ( $P > 0.05$ ) (Figure 1C). This interesting phenomenon probably was caused by hepatic  
193 TG potentially releasing into serum. Similarly, accumulation of hepatic TC was  
194 effectively alleviated by ACNs ( $P < 0.05$ ) (Figure 1D). The serum TC levels in MCD

195 + ACNs group showed an increasing trend but no significant differences compared to  
196 the MCD diet only group (Figure 1E).

197 **Amelioration of Steatohepatitis by ACNs.** The gross morphology of the livers in  
198 the control group displayed red and smooth tissue surface. After 4 weeks feeding with  
199 MCD diet, the gross morphology of livers appeared an obvious increase in tawny and  
200 brittle appearance, which was improved greatly by ACNs treatment (Figure 2A). The  
201 NAS calculation system was applied to semi-quantitatively evaluate the steatosis,  
202 inflammation and ballooning. Indeed, the histological analysis of H&E staining  
203 indicated significant microvesicular steatosis, inflammatory cell infiltration and  
204 hepatocyte ballooning in MCD diet group. However, livers of the ACNs-treated group  
205 exhibited only mild hepatic steatosis and effectively ameliorated inflammatory  
206 infiltration with reduction by 50% in hepatocyte ballooning compared to the MCD  
207 diet only group (Figure 2B-E).

208 **Inhibition of Liver Fibrosis by ACNs.** To assess the effect of ACNs on hepatic  
209 fibrosis, we carried out a Sirius Red staining of collagen in liver sections. A  
210 substantial increase in collagen deposition was observed in the MCD group compared  
211 with the control group. However, an obvious decrease in the stained area percentage  
212 was observed in the MCD + ACNs group (Figure 3A). Activation of hepatic stellate  
213 cells (HSCs), the major effectors in collagen production during hepatic fibrogenesis,  
214 is another indicator of fibrogenesis. To further evaluate HSCs activation,  
215 immunohistochemical staining of  $\alpha$ -SMA was performed. As displayed in Figure 3B,  
216 the data indicated that ACNs treatment reduced the expression of  $\alpha$ -SMA, suggestive

217 of inhibition of HSCs activation. Besides, both relative mRNA expression of collagen  
218 I and  $\alpha$ -SMA confirmed that ACNs played a suppressive effect on fibrosis in NASH  
219 (Figure 3C-D).

220 **Decrease of Oxidative Damage by ACNs.** Mitochondria are the major sites for  
221 ROS production. Quantitative evaluation of hepatic ROS is also an indicator of  
222 mitochondrial impairment. In our present study, the 4-week MCD diet up-regulated  
223 ROS levels of liver tissues by approximately 6-fold compared with the control diet  
224 and we unearthed that ACNs were able to significantly subdue ROS production  
225 induced by the MCD diet (Figure 4A-B). In addition, hepatic malondialdehyde (MDA)  
226 content, a widely used marker of oxidative stress, was increased by nearly 4-fold in  
227 the MCD group but only slightly increased in ACNs-treated mice (Figure 4C). The  
228 results of hepatic ROS and MDA levels clarified that ACNs played a suppressive  
229 effect on oxidative damage in NASH.

230 **Attenuation of Reduced Mitochondrial Content and Function by ACNs.** One of  
231 the common mitochondrial defects observed in NASH is depletion of mitochondrial  
232 DNA (mtDNA).<sup>4</sup> In our study, we first investigated the protective effect of ACNs on  
233 mtDNA. As shown in Figure 5A, mtDNA indeed displayed an apparent decrease in  
234 the MCD group, which was slightly improved through administration of ACNs ( $P <$   
235 0.05), though it was still lower than the number observed in the control group.  
236 Moreover, CPS-1, a hepatic mitochondrial membrane specific marker and a reflection  
237 of mitochondrial number and function in liver, declined in NASH but was  
238 significantly up-regulated by treatment of ACNs (Figure 5B-D).

**Enhancement of Mitochondrial Biogenesis by ACNs.** To investigate whether ACNs are capable of increasing mitochondrial biogenesis, we determined the relative mRNA expression of peroxisome proliferator-activated receptor-gamma coactivator-1 $\alpha$  (PGC-1 $\alpha$ ) and  $\beta$  (PGC-1 $\beta$ ), nuclear respiratory factor-1 (NRF-1) and 2 (NRF-2), and mitochondrial transcription factor A (Tfam) (pivotal regulators of mitochondrial biogenesis). As displayed in Figure 6A and B, PGC-1 $\alpha$  dropped in NASH ( $P < 0.05$ ) but exhibited sharply increased expression after ACNs intervention, whereas PGC-1 $\beta$  was unaffected by either MCD diet or ACNs treatment. In addition, there was almost 50% reduction in PGC-1 $\alpha$ -target genes NRF-1, NRF-2 and TFAM following a MCD diet, while the reduction was effectively suppressed with treatment of ACNs. Likewise, immunoblotting analysis revealed that ACNs reversed the reduction of protein abundance of PGC-1 $\alpha$  induced by the MCD diet, while no significant difference in PGC-1 $\beta$  expression was observed among the three groups (Figure 6C). Together, these results indicate that ACNs may induce mitochondrial biogenesis through PGC-1 $\alpha$  pathway.

Our previous research has demonstrated activation of AMPK by ACNs in hepatocytes,<sup>14</sup> which could result in phosphorylation of the transcriptional coactivator PGC-1 $\alpha$  thus leading to increased mitochondrial biogenesis.<sup>23,24</sup> Then, we determined the protein levels of p-AMPK and total AMPK and discovered an over 50% decrease in p-AMPK in the liver of NASH mice, which was rescued by ACNs with no change of total AMPK (Figure 6C).

**Amelioration of Mitochondrial Electron Transfer Chain (ETC) Defects by**

261 **ACNs.** Mitochondrial ETC is constituted of four respiratory complexes (Complex I to  
262 IV).<sup>25</sup> To confirm the alteration of mitochondrial ETC and effects of ACNs on it at a  
263 functional level, the protein expression of two major sites of electron input into the  
264 electron transport system (Complex I and IV) in total liver lysates was examined  
265 (Figure 6D). The mice fed the MCD diet had mitochondrial ETC defects, as shown by  
266 conspicuously diminished protein expression of mitochondrial Complexes I and V,  
267 especially the Complexes IV (approximately 4-fold). As expected, dietary ACNs  
268 intervention successfully intensified protein expression of mitochondrial Complexes I  
269 and V, reflecting improvement of mitochondrial oxidative phosphorylation and  
270 enhancement of mitochondrial biogenesis and function.

271 **Improvement of Mitochondrial  $\beta$ -Oxidation by ACNs.** Impairment of  
272 mitochondrial oxidative phosphorylation is often followed by inhibition of  
273 mitochondrial fatty acid  $\beta$ -oxidation. In the present study, we indeed discovered that  
274 both protein and mRNA expression of peroxisome proliferator-activated receptor- $\alpha$   
275 (PPAR- $\alpha$ ) were nearly halved in NASH but was successfully restored by ACNs  
276 intervention (Figure 6C and E). PPAR- $\alpha$  is one of a superfamily of nuclear hormone  
277 receptors and able to transcriptionally up-regulate nuclear genes encoding  
278 mitochondrial fatty acid oxidation enzymes.<sup>26</sup> We then determined gene expression  
279 levels of carnitine palmitoyltransferase 1 (CPT-1) and medium chain acyl CoA  
280 dehydrogenase (MCAD), two rate-limiting enzymes of fatty acids  $\beta$ -oxidation. As  
281 illustrated in Figure 6E, relative mRNA expression of CPT-1 and MCAD dropped  
282 significantly in NASH ( $P < 0.05$ ), however, both were augmented with administration



of ACNs. These were accompanied with no distinction of fatty acid synthesis (FAS) between the groups. Thus, ACNs seemed to be able to stimulate hepatic lipid oxidation, leading to reduction of TG accumulation within hepatocytes.

## DISCUSSION

Previously, we and others have shown that ACNs have hepatoprotective activities in obese and diabetic rodents.<sup>16,27</sup> In the present study, we demonstrated that purified ACNs from bilberry and black currant were capable of ameliorating hepatic steatosis, inflammation, oxidative stress as well as signs of fibrosis and improving depletion of mitochondrial content and damage of mitochondrial biogenesis, ETC as well as  $\beta$ -oxidation. To our knowledge, this work provides the first evidence that ACNs, the soluble flavonoids, alleviate complications of NASH and improve degeneration of mitochondrial function in mice fed a MCD diet.

Many researches certificate that abnormalities in the number and quality of mitochondria are frequently observed in NASH and involved in its pathogenesis. These mitochondrial abnormalities include ultrastructural lesions, depletion of mtDNA, reduction of respiratory chain activity, impairment of mitochondrial  $\beta$ -oxidation and induction of uncoupling and apoptosis.<sup>28</sup> As expected, our MCD diet-induced NASH model displayed a reduction in mitochondrial content, as well as impairment of mitochondrial biogenesis, ETC activity and  $\beta$ -oxidation function.

In our study, we discovered that dietary supplement of ACNs could ameliorate the depletion of mtDNA and decrease expression of CPS-1 (Figure 5). Mitochondrial DNA represents mitochondrial self-replication and is involved in mitochondrial

305 biogenesis.<sup>24</sup> It is also crucial for mitochondrial oxidative phosphorylation, encoding  
306 thirteen MRC polypeptides that embed within complexes I, III, IV, and V, and further  
307 for  $\beta$ -oxidation.<sup>29</sup> CPS-1, a hepatic mitochondrial membrane-specific marker,  
308 qualitatively reflects hepatic mitochondrial content and function in the liver and is a  
309 comprehensive marker of mitochondrial damage.<sup>30</sup> It could be concluded from our  
310 work that dietary ACNs mitigate the depletion of mitochondrial content and  
311 dysfunction in NASH.

312 Mitochondrial biogenesis plays a critical role in maintaining the dynamic  
313 equilibrium of proliferation and degradation of mitochondria in hepatocytes.<sup>31</sup>  
314 Activation of mitochondrial biogenesis is mainly reflected by the activation of NRF-1  
315 and NRF-2, which conversely regulates the expression of Tfam, a protein essential for  
316 transcription, replication and maintenance of the mtDNA. In our study, the mRNA  
317 expression of NRF-1, NRF-2 and Tfam was significantly decreased in mice fed the  
318 MCD diet, indicating damage to mitochondrial biogenesis. This effect was evidently  
319 ameliorated by administration of ACNs, especially with respect to NRF-2 and Tfam  
320 (Figure 6B). These data suggest that ACNs stimulate mitochondrial biogenesis in  
321 NASH.

322 As major sites for cellular respiration, mitochondria play a vital role in maintaining  
323 energy metabolism and function of hepatocytes, which includes citric acid cycle and  
324 oxidative phosphorylation process. The oxidative phosphorylation process of ETC is  
325 located on inner membrane of mitochondrion and consisted of four large  
326 trans-membrane protein complexes (mitochondrial respiratory Complex I, II, III and

327 IV).<sup>25</sup> Complex I and IV are two important and major protein complexes of electron  
328 transfer chain among the four. Via determination of the two representative protein  
329 complexes, we ascertained that ETC defects happened in mice fed the MCD diet  
330 which, however, were visibly alleviated by ACNs administration (Figure 6D).

331 One of the most common hepatic cell injuries is the result of accumulation of  
332 various lipids, which further contributes to development and progression of fatty liver.  
333 The main mechanisms are as follows: increased fatty acid uptake and *de novo* hepatic  
334 lipogenesis, decreased fatty acid  $\beta$ -oxidation and hepatic very low density  
335 lipoprotein-triglyceride (VLDL) secretion. One of the mechanisms of NASH induced  
336 by the MCD diet is decreased VLDL assembly and secretion, contributing to  
337 disturbance in phosphatidylcholine synthesis that is caused by deficiencies in  
338 methionine and choline.<sup>32</sup> In our study, we also observed that this model was  
339 accompanied by impairment of mitochondrial  $\beta$ -oxidation, manifested by decrease in  
340 gene or protein expression of PPAR- $\alpha$ , CPT-1 and MCAD (Figure 6C and E), which  
341 consequently cooperated with decreased VLDL to result in the reduction of lipid  
342 clearance. Our data show that ACNs treatment significantly up-regulated protein  
343 expression of PPAR- $\alpha$  and gene expression of PPAR- $\alpha$ , CPT-1 and MCAD (Figure  
344 6E). PPAR- $\alpha$  is predominantly expressed in the liver where it transcriptionally  
345 up-regulates nuclear genes encoding mitochondrial fatty acid oxidation enzymes  
346 CPT-1 and MCAD.<sup>26</sup> CPT-1 locates on the outer mitochondrial membrane and is a  
347 key rate-limiting enzyme of long-chain fatty acid  $\beta$ -oxidation while MCAD is a key  
348 enzyme in the first step of medium-chain fatty acid  $\beta$ -oxidation. We conclude that

349 ACNs can improve impairment of mitochondrial  $\beta$ -oxidation in NASH induced by the  
350 MCD diet, which further counteracts hepatocyte injury resulting from lipid  
351 accumulation by promoting TG clearance.

352 In line with existing research illustrating that ACNs are able to activate protein  
353 expression of AMPK *in vitro*<sup>14</sup> and *in vivo*,<sup>16</sup> we also found that ACNs could attenuate  
354 the reduction of p-AMPK expression induced by the MCD diet (but not total AMPK;  
355 Figure 6C). Moreover, emerging evidence showed that the activation of AMPK leads  
356 to increased expression of the downstream molecule PGC-1 $\alpha$ ,<sup>33</sup> which was  
357 demonstrated to be a potent stimulator of mitochondrial biogenesis in liver, heart and  
358 skeletal muscle by contributing to activation of NRF-1, NRF-2 and Tfam.<sup>34</sup> In the  
359 present study, we showed that protein and gene expressions of PGC-1 $\alpha$  and its target  
360 genes were up-regulated by ACNs, which subsequently potentiated mitochondrial  
361 biogenesis. These data suggest that the improvement of mitochondrial dysfunction  
362 induced by ACNs treatment is attributed to increased phosphorylation of AMPK,  
363 which subsequently increased expression of PGC-1 $\alpha$ , rather than PGC-1 $\beta$  (Figure 6A  
364 and C).

365 In summary, our study shows that ACNs ameliorate liver disease in steatohepatitis  
366 progression and improve mitochondrial defects. Our previous study also showed that  
367 anthocyanin cyanidin 3-*O*- $\beta$ -glucoside could notably improve mitochondrial function  
368 in high glucose-stressed hepatocytes.<sup>35</sup> Considering previous studies reporting that  
369 mitochondrial dysfunction takes precedence over insulin resistance and hepatic  
370 steatosis and leads to the natural history of NAFLD<sup>30,36</sup> and combining with our own

371 results, we venture to conclude that administration of ACNs attenuated NASH due to  
372 the improvement of mitochondrial dysfunction in mice fed a MCD diet. The possible  
373 mechanism may involve activation of AMPK/PGC-1 $\alpha$  signaling axis by ACNs, which  
374 subsequently contributes to improvement of depletion of mitochondrial mtDNA and  
375 mitochondrial biogenesis function, improves ECT activity and  $\beta$ -oxidation, and  
376 eventually attenuates lipid accumulation-induced hepatocyte injury by enhancing TG  
377 clearance. Due to limitations such as the animal model of NASH and lack of  
378 inhibitors or blockers in our current study, further research is needed to investigate the  
379 detailed molecular mechanisms and potential clinical applications of ACNs in  
380 NAFLD.

#### 381 **ABBREVIATIONS USED**

382  $\alpha$ -SMA, alpha smooth muscle actin; ACNs, anthocyanins; ALT, alanine  
383 aminotransferase; AMPK, AMP-activated protein kinase; AST, aspartate  
384 aminotransferase; Complex I, nicotinamide adenine dinucleotide dehydrogenase;  
385 Complex IV, cytochrome c oxidase; CPS-1, carbamoyl phosphate synthase 1; CPT-1,  
386 carnitine palmitoyltransferase 1; DHE, dihydroethidium; ETC, electron transfer chain;  
387 FAS, fatty acid synthesis; H&E, hematoxylin and eosin; HSC, hepatic stellate cell;  
388 MCAD, medium chain acyl CoA dehydrogenase; MCD, methionine-choline-deficient  
389 diet; MDA, malondialdehyde; MRC, mitochondrial respiratory chain; mtDNA,  
390 mitochondrial DNA; NAFLD, nonalcoholic fatty liver disease; NAS, nonalcoholic  
391 fatty liver disease activity scoring; NASH, nonalcoholic steatohepatitis; NRF-1/2,  
392 nuclear respiratory factor-1/2; p-AMPK, phosphorylated AMP-activated protein

kinase; PGC-1 $\alpha/\beta$ , peroxisome proliferator-activated receptor-gamma  
coactivator-1 $\alpha/\beta$ ; PPAR- $\alpha$ , peroxisome proliferator-activated receptor- $\alpha$ ; ROS,  
reactive oxygen species; TC, total cholesterol; Tfam, transcription factor A; TG,  
triglyceride; VLDL, very low density lipoprotein-triglyceride

## ACKNOWLEDGEMENTS

This work was funded by grants from the National Basic Research Program (973  
Program, 2012CB517506), the National Nature Science Foundation (81172655,  
81372994) and China Scholarship Council (201308440005).

## SUPPORTING INFORMATION

Additional information (Table S1-S3). This material is available free of charge via the  
Internet at <http://pubs.acs.org>.

## REFERENCES

- (1) Shen, H. C.; Zhao, Z. H.; Hu, Y. C.; Chen, Y. F.; Tung, T. H. Relationship  
between obesity, metabolic syndrome, and nonalcoholic fatty liver disease in the  
elderly agricultural and fishing population of Taiwan. *Clin. Interv. Aging* **2014**, *9*,  
501-508.
- (2) Tiniakos, D. G.; Vos, M. B.; Brunt, E. M. Nonalcoholic fatty liver disease:  
pathology and pathogenesis. *Annu. Rev. Pathol.* **2010**, *5*, 145-171.
- (3) Caldwell, S. H.; Chang, C. Y.; Nakamoto, R. K.; Krugner-Higby, L.  
Mitochondria in nonalcoholic fatty liver disease. *Clin. Liver Dis.* **2004**, *8*, 595-617, x.
- (4) Sobaniec-Lotowska, M. E.; Lebensztejn, D. M. Ultrastructure of hepatocyte  
mitochondria in nonalcoholic steatohepatitis in pediatric patients: usefulness of

415 electron microscopy in the diagnosis of the disease. *Am. J. Gastroenterol.* **2003**, *98*,  
416 1664-1665.

417 (5) Perez-Carreras, M.; Del Hoyo, P.; Martin, M. A.; Rubio, J. C.; Martin, A.;  
418 Castellano, G.; Colina, F.; Arenas, J.; Solis-Herruzo, J. A. Defective hepatic  
419 mitochondrial respiratory chain in patients with nonalcoholic steatohepatitis.  
420 *Hepatology* **2003**, *38*, 999-1007.

421 (6) Finocchietto, P. V.; Holod, S.; Barreyro, F.; Peralta, J. G.; Alippe, Y.;  
422 Giovambattista, A.; Carreras, M. C.; Poderoso, J. J. Defective leptin-AMP-dependent  
423 kinase pathway induces nitric oxide release and contributes to mitochondrial  
424 dysfunction and obesity in ob/ob mice. *Antioxid. Redox. Signal* **2011**, *15*, 2395-2406.

425 (7) Roglans, N.; Vila, L.; Farre, M.; Alegret, M.; Sanchez, R. M.;  
426 Vazquez-Carrera, M.; Laguna, J. C. Impairment of hepatic Stat-3 activation and  
427 reduction of PPARalpha activity in fructose-fed rats. *Hepatology* **2007**, *45*, 778-788.

428 (8) Serviddio, G.; Giudetti, A. M.; Bellanti, F.; Priore, P.; Rollo, T.; Tamborra, R.;  
429 Siculella, L.; Vendemiale, G.; Altomare, E.; Gnoni, G. V. Oxidation of hepatic  
430 carnitine palmitoyl transferase-I (CPT-I) impairs fatty acid beta-oxidation in rats fed a  
431 methionine-choline deficient diet. *PLoS One* **2011**, *6*, e24084.

432 (9) Kuo, J. J.; Chang, H. H.; Tsai, T. H.; Lee, T. Y. Positive effect of curcumin on  
433 inflammation and mitochondrial dysfunction in obese mice with liver steatosis. *Int. J.*  
434 *Mol. Med.* **2012**, *30*, 673-679.

435 (10) Marcolin, E.; San-Miguel, B.; Vallejo, D.; Tieppo, J.; Marroni, N.;  
436 Gonzalez-Gallego, J.; Tunon, M. J. Quercetin treatment ameliorates inflammation and

- 437 fibrosis in mice with nonalcoholic steatohepatitis. *J. Nutr.* **2012**, *142*, 1821-1828.
- 438 (11) Shih, P. H.; Hwang, S. L.; Yeh, C. T.; Yen, G. C. Synergistic effect of  
439 cyanidin and PPAR agonist against nonalcoholic steatohepatitis-mediated oxidative  
440 stress-induced cytotoxicity through MAPK and Nrf2 transduction pathways. *J. Agric.*  
441 *Food Chem.* **2012**, *60*, 2924-2933.
- 442 (12) Masterjohn, C.; Bruno, R. S. Therapeutic potential of green tea in  
443 nonalcoholic fatty liver disease. *Nutr. Rev.* **2012**, *70*, 41-56.
- 444 (13) Liu, Y.; Wang, D.; Zhang, D.; Lv, Y.; Wei, Y.; Wu, W.; Zhou, F.; Tang, M.;  
445 Mao, T.; Li, M.; Ji, B. Inhibitory effect of blueberry polyphenolic compounds on oleic  
446 acid-induced hepatic steatosis in vitro. *J. Agric. Food Chem.* **2011**, *59*, 12254-12263.
- 447 (14) Guo, H.; Liu, G.; Zhong, R.; Wang, Y.; Wang, D.; Xia, M.  
448 Cyanidin-3-O-beta-glucoside regulates fatty acid metabolism via an AMP-activated  
449 protein kinase-dependent signaling pathway in human HepG2 cells. *Lipids Health.*  
450 *Dis.* **2012**, *11*, 10.
- 451 (15) Chang, J. J.; Hsu, M. J.; Huang, H. P.; Chung, D. J.; Chang, Y. C.; Wang, C. J.  
452 Mulberry anthocyanins inhibit oleic acid induced lipid accumulation by reduction of  
453 lipogenesis and promotion of hepatic lipid clearance. *J. Agric. Food Chem.* **2013**, *61*,  
454 6069-6076.
- 455 (16) Hwang, Y. P.; Choi, J. H.; Han, E. H.; Kim, H. G.; Wee, J. H.; Jung, K. O.;  
456 Jung, K. H.; Kwon, K. I.; Jeong, T. C.; Chung, Y. C.; Jeong, H. G. Purple sweet potato  
457 anthocyanins attenuate hepatic lipid accumulation through activating adenosine  
458 monophosphate-activated protein kinase in human HepG2 cells and obese mice. *Nutr.*



459 *Res.* **2011**, *31*, 896-906.

460 (17) Cho, B. O.; Ryu, H. W.; Jin, C. H.; Choi, D. S.; Kang, S. Y.; Kim, D. S.;  
461 Byun, M. W.; Jeong, I. Y. Blackberry extract attenuates oxidative stress through  
462 up-regulation of Nrf2-dependent antioxidant enzymes in carbon tetrachloride-treated  
463 rats. *J. Agric. Food Chem.* **2011**, *59*, 11442-11448.

464 (18) Zhang, Z. F.; Lu, J.; Zheng, Y. L.; Wu, D. M.; Hu, B.; Shan, Q.; Cheng, W.;  
465 Li, M. Q.; Sun, Y. Y. Purple sweet potato color attenuates hepatic insulin resistance  
466 via blocking oxidative stress and endoplasmic reticulum stress in high-fat-diet-treated  
467 mice. *J. Nutr. Biochem.* **2013**, *24*, 1008-1018.

468 (19) Qin, Y.; Xia, M.; Ma, J.; Hao, Y.; Liu, J.; Mou, H.; Cao, L.; Ling, W.  
469 Anthocyanin supplementation improves serum LDL- and HDL-cholesterol  
470 concentrations associated with the inhibition of cholesteryl ester transfer protein in  
471 dyslipidemic subjects. *Am. J. Clin. Nutr.* **2009**, *90*, 485-492.

472 (20) Kleiner, D. E.; Brunt, E. M.; Van Natta, M.; Behling, C.; Contos, M. J.;  
473 Cummings, O. W.; Ferrell, L. D.; Liu, Y. C.; Torbenson, M. S.; Unalp-Arida, A.; Yeh,  
474 M.; McCullough, A. J.; Sanyal, A. J. Design and validation of a histological scoring  
475 system for nonalcoholic fatty liver disease. *Hepatology* **2005**, *41*, 1313-1321.

476 (21) Luo, X.; Xiao, Y.; Song, F.; Yang, Y.; Xia, M.; Ling, W. Increased plasma  
477 S-adenosyl-homocysteine levels induce the proliferation and migration of VSMCs  
478 through an oxidative stress-ERK1/2 pathway in apoE(-/-) mice. *Cardiovasc. Res.*  
479 **2012**, *95*, 241-250.

480 (22) Aoyama, T.; Hida, K.; Kuroda, S.; Seki, T.; Yano, S.; Shichinohe, H.; Iwasaki,

- 481 Y. Edaravone (MCI-186) scavenges reactive oxygen species and ameliorates tissue  
482 damage in the murine spinal cord injury model. *Neurol. Med. Chir. (Tokyo)* **2008**, *48*,  
483 539-545.
- 484 (23) Steinberg, G. R.; Kemp, B. E. AMPK in Health and Disease. *Physiol. Rev.*  
485 **2009**, *89*, 1025-1078.
- 486 (24) Hock, M. B.; Kralli, A. Transcriptional control of mitochondrial biogenesis  
487 and function. *Annu. Rev. Physiol.* **2009**, *71*, 177-203.
- 488 (25) Ruiz, L. M.; Jensen, E. L.; Bustos, R. I.; Arguello, G.; Gutierrez-Garcia, R.;  
489 Gonzalez, M.; Hernandez, C.; Paredes, R.; Simon, F.; Riedel, C.; Ferrick, D.; Elorza,  
490 A. A. Adaptive responses of mitochondria to mild copper deprivation involve changes  
491 in morphology, OXPHOS remodeling and bioenergetics. *J. Cell. Physiol.* **2014**, *229*,  
492 607-619.
- 493 (26) Mandard, S.; Muller, M.; Kersten, S. Peroxisome proliferator-activated  
494 receptor alpha target genes. *Cell Mol. Life Sci.* **2004**, *61*, 393-416.
- 495 (27) Guo, H.; Xia, M.; Zou, T.; Ling, W.; Zhong, R.; Zhang, W. Cyanidin  
496 3-glucoside attenuates obesity-associated insulin resistance and hepatic steatosis in  
497 high-fat diet-fed and *db/db* mice via the transcription factor FoxO1. *J. Nutr. Biochem.*  
498 **2012**, *23*, 349-360.
- 499 (28) Begriche, K.; Massart, J.; Robin, M. A.; Bonnet, F.; Fromenty, B.  
500 Mitochondrial adaptations and dysfunctions in nonalcoholic fatty liver disease.  
501 *Hepatology* **2013**, *58*, 1497-1507.
- 502 (29) Begriche, K.; Massart, J.; Robin, M. A.; Borgne-Sanchez, A.; Fromenty, B.

503 Drug-induced toxicity on mitochondria and lipid metabolism: mechanistic diversity  
504 and deleterious consequences for the liver. *J. Hepatol.* **2011**, *54*, 773-794.

505 (30) Rector, R. S.; Thyfault, J. P.; Uptergrove, G. M.; Morris, E. M.; Naples, S. P.;  
506 Borengasser, S. J.; Mikus, C. R.; Laye, M. J.; Laughlin, M. H.; Booth, F. W.; Ibdah, J.  
507 A. Mitochondrial dysfunction precedes insulin resistance and hepatic steatosis and  
508 contributes to the natural history of non-alcoholic fatty liver disease in an obese  
509 rodent model. *J. Hepatol.* **2010**, *52*, 727-736.

510 (31) Kubli, D. A.; Gustafsson, A. B. Mitochondria and mitophagy: the yin and  
511 yang of cell death control. *Circ. Res.* **2012**, *111*, 1208-1221.

512 (32) Anstee, Q. M.; Goldin, R. D. Mouse models in non-alcoholic fatty liver  
513 disease and steatohepatitis research. *Int. J. Exp. Pathol.* **2006**, *87*, 1-16.

514 (33) Lee, W. J.; Kim, M.; Park, H. S.; Kim, H. S.; Jeon, M. J.; Oh, K. S.; Koh, E.  
515 H.; Won, J. C.; Kim, M. S.; Oh, G. T.; Yoon, M.; Lee, K. U.; Park, J. Y. AMPK  
516 activation increases fatty acid oxidation in skeletal muscle by activating PPARalpha  
517 and PGC-1. *Biochem. Biophys. Res. Commun.* **2006**, *340*, 291-295.

518 (34) Scarpulla, R. C.; Vega, R. B.; Kelly, D. P. Transcriptional integration of  
519 mitochondrial biogenesis. *Trends. Endocrinol. Metab.* **2012**, *23*, 459-466.

520 (35) Jiang, X.; Tang, X.; Zhang, P.; Liu, G.; Guo, H. Cyanidin-3-O-beta-glucoside  
521 protects primary mouse hepatocytes against high glucose-induced apoptosis by  
522 modulating mitochondrial dysfunction and the PI3K/Akt pathway. *Biochem.*  
523 *Pharmacol.* **2014**, *90*, 135-144.

524 (36) Lee, S. J.; Zhang, J.; Choi, A. M.; Kim, H. P. Mitochondrial dysfunction

525 induces formation of lipid droplets as a generalized response to stress. *Oxid. Med.*

526 *Cell Longev.* **2013**, 2013, 327167.

527

## Figure Captions

**Figure 1.** ACNs decreased lipid accumulation in mice fed the MCD diet. (A) Frozen sections (5  $\mu\text{m}$  thick) were stained with Oil Red O, which marked neutral lipid. Representative micrographs (200  $\times$  magnification) are shown. (B-E) TG and TC levels were measured from all frozen liver specimens and serum. Values are expressed as mean  $\pm$  SD,  $n = 8$ .  $*P < 0.05$  versus the control group;  $^{\#}P < 0.05$  versus the MCD group.

**Figure 2.** ACNs ameliorated steatohepatitis induced by the MCD diet. (A) Representative gross morphology images are shown. (B) Hepatic histological analysis of H&E staining (200  $\times$  magnification). Inflammatory infiltration (black arrow) and hepatocyte ballooning (red arrow) were observed in liver sections from the MCD group which were improved in the ACNs-treated group. (C-E) Histological NAS scores of liver tissues. Values are expressed as mean  $\pm$  SD,  $n = 8$ .  $*P < 0.05$  versus the control group;  $^{\#}P < 0.05$  versus the MCD group.

**Figure 3.** ACNs played an inhibitory role in progression of fibrosis in mice fed an MCD diet. (A) Paraffin-embedded liver specimens were stained with Sirius Red and observed by light microscopy. (B) Paraffin sections were immunoassayed for fibrosis markers,  $\alpha$ -SMA (black arrows), to assess hepatic stellate cells activation. Representative photographs (200  $\times$  magnification) are shown. (C-D) Total RNA was isolated from the livers and genes expression of collagen I and  $\alpha$ -SMA were

subjected to RT-PCR analysis, the control group was set to be 1. Values are expressed as mean  $\pm$  SD,  $n = 8$ .  $*P < 0.05$  versus the control group;  $^{\#}P < 0.05$  versus the MCD group.

**Figure 4.** ACNs decreased oxidative damage in NASH. (A) Frozen sections of livers were stained with fluorescent probe DHE, showing red fluorescence in regions of ROS production. Representative fluorescence micrographs ( $200 \times$  magnification) are shown. (B) Fluorescent densitometry of DHE staining was quantified by ImageJ software. (C) MDA content in livers. Values are expressed as mean  $\pm$  SD,  $n = 8$ .  $*P < 0.05$  versus the control group;  $^{\#}P < 0.05$  versus the MCD group.

**Figure 5.** ACNs attenuated reduction of mitochondrial content and function in NASH. (A) Mitochondrial genome copy number was shown as the ratio of mtDNA to nDNA from purified liver DNA, which was determined by quantitative real-time PCR. The control group was set to be 1. (B) Representative immunofluorescent photomicrographs ( $200 \times$  magnification) for mitochondrial marker CPS-1 (red fluorescence) showed granular staining patterns in liver frozen sections. (C) Fluorescent staining of CPS-1 per field was quantified by Image J software and reported as mean integrated density. (D) Western blot analysis was performed to semi-quantitatively assess expression levels of CPS-1 from liver homogenates. The control group was set to be 1. Values are expressed as mean  $\pm$  SD,  $n = 8$ .  $*P < 0.05$  versus the control group;  $^{\#}P < 0.05$  versus the MCD group.

**Figure 6.** ACNs stimulated mitochondrial biogenesis and improved mitochondrial ETC defects as well as enhanced mitochondrial  $\beta$ -oxidation in NASH. (A-B) Real-time PCR was applied to measure mRNA expression of PGC-1 $\alpha$  and PGC-1 $\beta$  (A) and genes related to mitochondrial biogenesis (NRF-1, NRF-2 and Tfam) (B). (C) Protein expression of p-AMPK, total AMPK, PGC-1 $\alpha$ , PGC-1 $\beta$  and PPAR- $\alpha$  in livers were measured by Western blot, quantified using densitometry and normalized by GAPDH content. (D) Protein levels of Complex I and IV were examined by Western blot. (E) Genes related to fatty acid oxidation (CPT-1, MCAD and PPAR- $\alpha$ ) and lipogenesis (FAS) were subjected to RT-PCR analysis. The control group was set to be 1. Results are expressed as mean  $\pm$  SD, n = 6-8. \* $P$  < 0.05 versus the control group; # $P$  < 0.05 versus the MCD group.

**Table 1:** Animal characteristics and serum liver enzymes of mice in different study groups<sup>a</sup>

	Control	MCD	MCD + ACNs
<b>Initial body weight (g)</b>	25.12 ± 1.30	25.09 ± 1.26	25.35 ± 1.20
<b>Final body weight (g)</b>	27.39 ± 2.74	16.93 ± 0.73*	17.19 ± 0.42*
<b>Liver weight (g)</b>	0.89 ± 0.13	0.54 ± 0.06*	0.56 ± 0.10*
<b>Liver to body weight ratio (%)</b>	3.53 ± 0.62	3.20 ± 0.20	3.40 ± 0.34
<b>Serum ALT level (U/L)</b>	6.03 ± 1.68	79.08 ± 36.54*	58.65 ± 25.03* <sup>#</sup>
<b>Serum AST level (U/L)</b>	23.43 ± 1.66	49.48 ± 3.17*	40.26 ± 2.07* <sup>#</sup>

<sup>a</sup>All values are mean ± SD, n = 8. Statistical analysis of the data for multiple comparisons was performed by ANOVA. \**P* < 0.05 versus the control group; <sup>#</sup>*P* < 0.05 versus the MCD group.



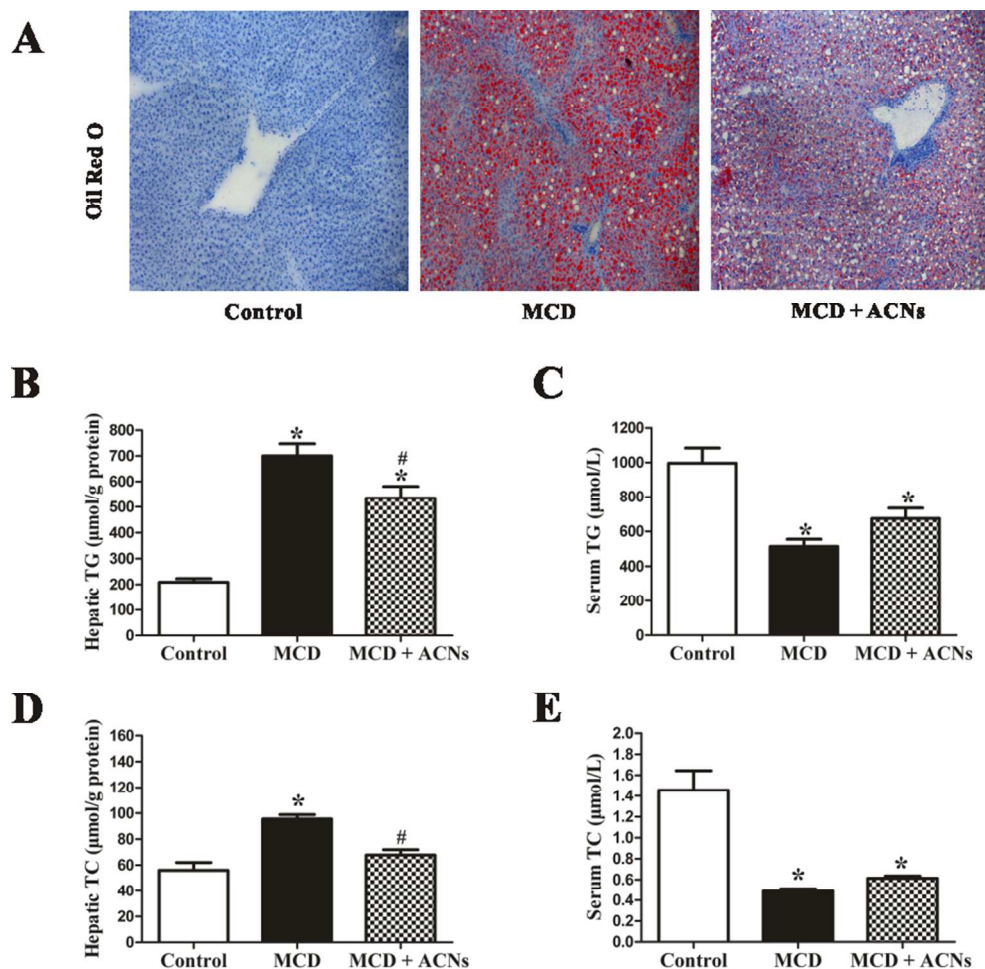


Figure 1. ACNs decreased lipid accumulation in mice fed the MCD diet. (A) Frozen sections (5  $\mu\text{m}$  thick) were stained with Oil Red O, which marked neutral lipid. Representative micrographs (200  $\times$  magnification) are shown. (B-E) TG and TC levels were measured from all frozen liver specimens and serum. Values are expressed as mean  $\pm$  SD,  $n = 8$ . \* $P < 0.05$  versus the control group; #  $P < 0.05$  versus the MCD group.

79x77mm (300  $\times$  300 DPI)

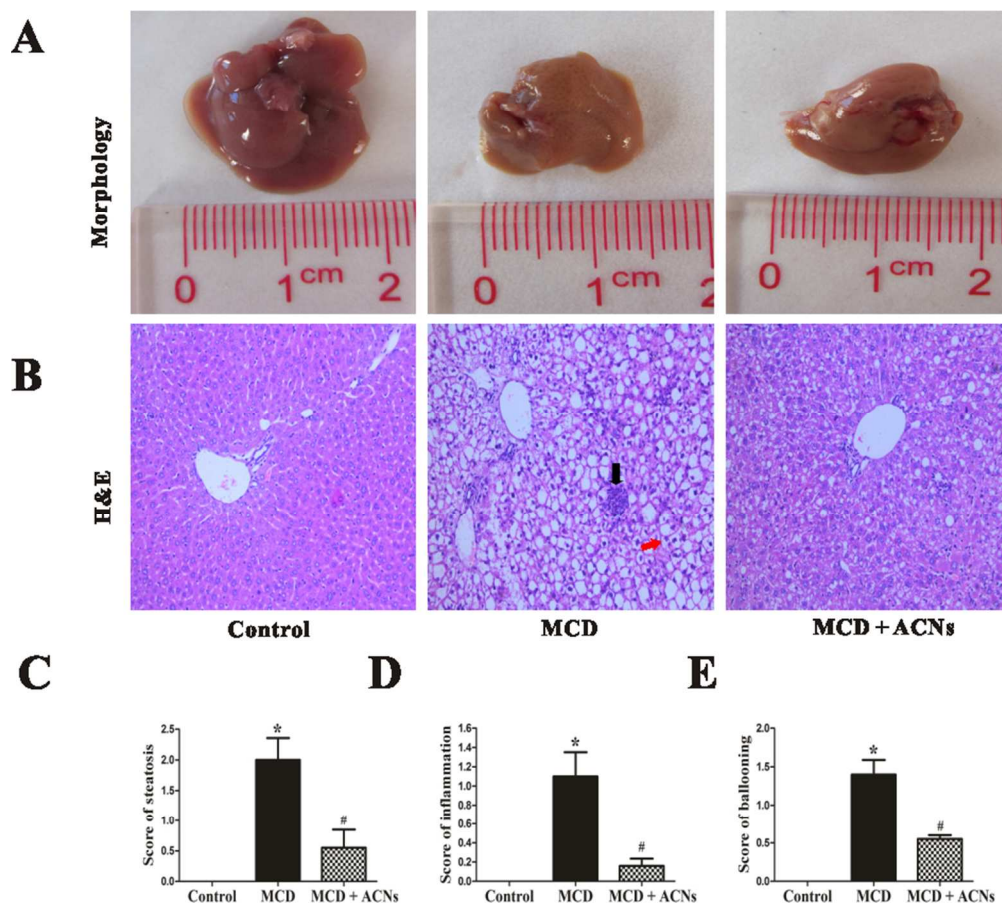


Figure 2. ACNs ameliorated steatohepatitis induced by the MCD diet. (A) Representative gross morphology images are shown. (B) Hepatic histological analysis of H&E staining (200 × magnification). Inflammatory infiltration (black arrow) and hepatocyte ballooning (red arrow) were observed in liver sections from the MCD group which were improved in the ACNs-treated group. (C-E) Histological NAS scores of liver tissues. Values are expressed as mean ± SD, n = 8. \*P < 0.05 versus the control group; #P < 0.05 versus the MCD group.

79x72mm (300 × 300 DPI)

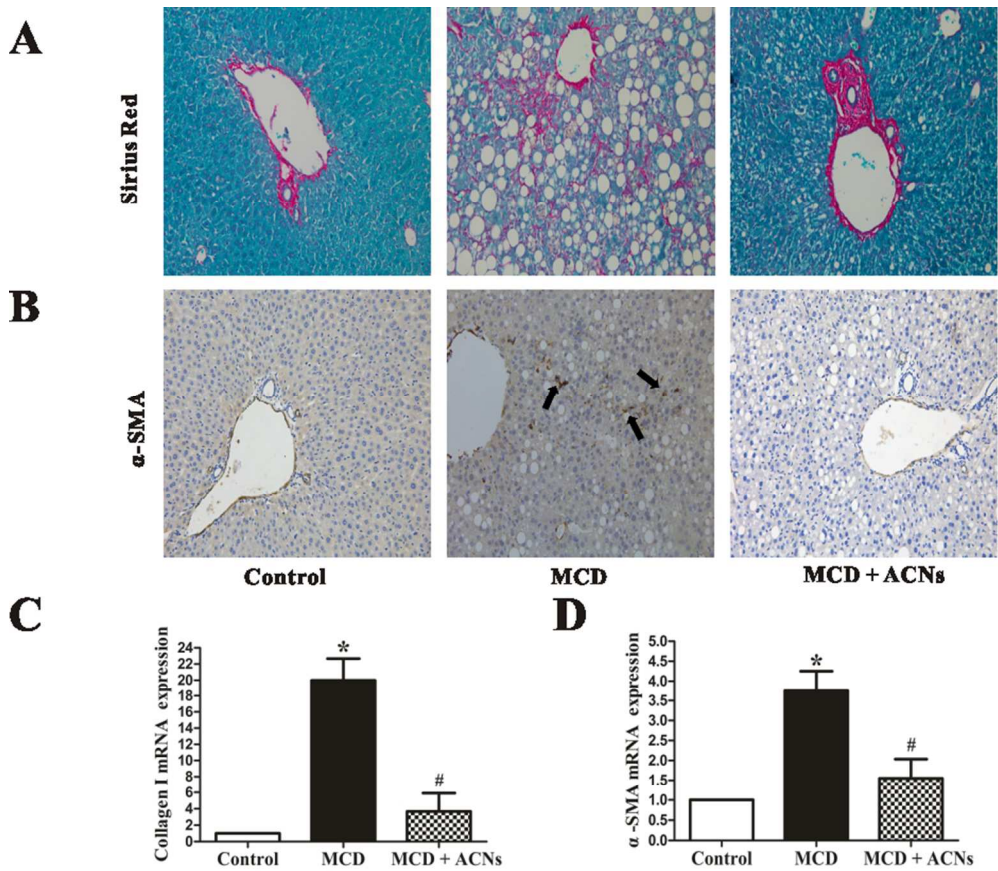


Figure 3. ACNs played an inhibitory role in progression of fibrosis in mice fed an MCD diet. (A) Paraffin-embedded liver specimens were stained with Sirius Red and observed by light microscopy. (B) Paraffin sections were immunoassayed for fibrosis markers,  $\alpha$ -SMA (black arrows), to assess hepatic stellate cells activation. Representative photographs (200  $\times$  magnification) are shown. (C-D) Total RNA was isolated from the livers and genes expression of collagen I and  $\alpha$ -SMA were subjected to RT-PCR analysis, the control group was set to be 1. Values are expressed as mean  $\pm$  SD, n = 8. \*P < 0.05 versus the MCD group; #P < 0.05 versus the control group; 79x69mm (300  $\times$  300 DPI)

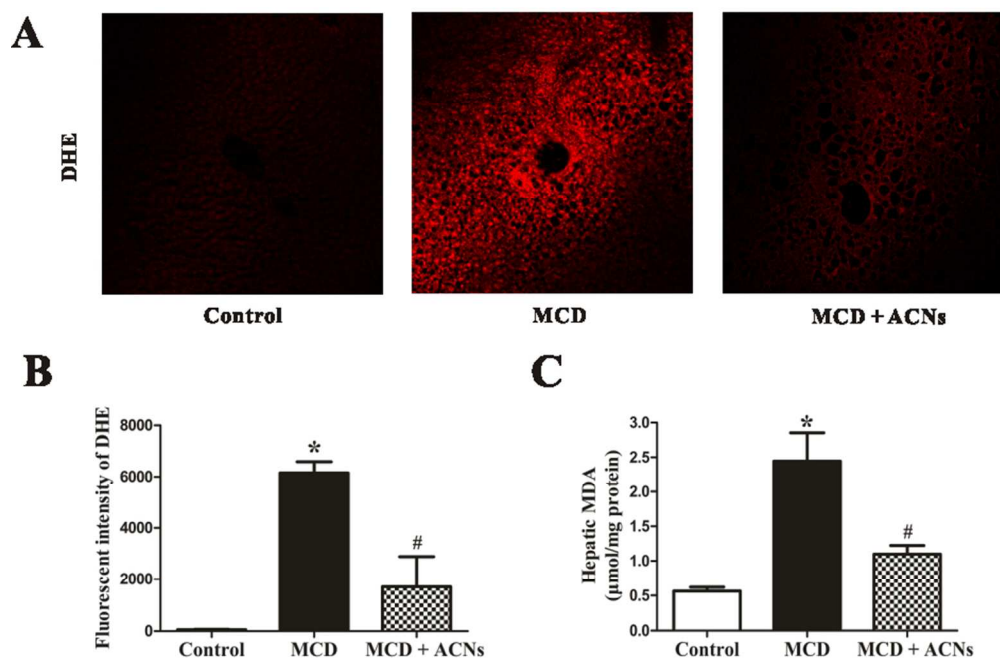


Figure 4. ACNs decreased oxidative damage in NASH. (A) Frozen sections of livers were stained with fluorescent probe DHE, showing red fluorescence in regions of ROS production. Representative fluorescence micrographs (200  $\times$  magnification) are shown. (B) Fluorescent densitometry of DHE staining was quantified by ImageJ software. (C) MDA content in livers. Values are expressed as mean  $\pm$  SD,  $n = 8$ . \* $P < 0.05$  versus the control group; # $P < 0.05$  versus the MCD group.

79x53mm (300  $\times$  300 DPI)



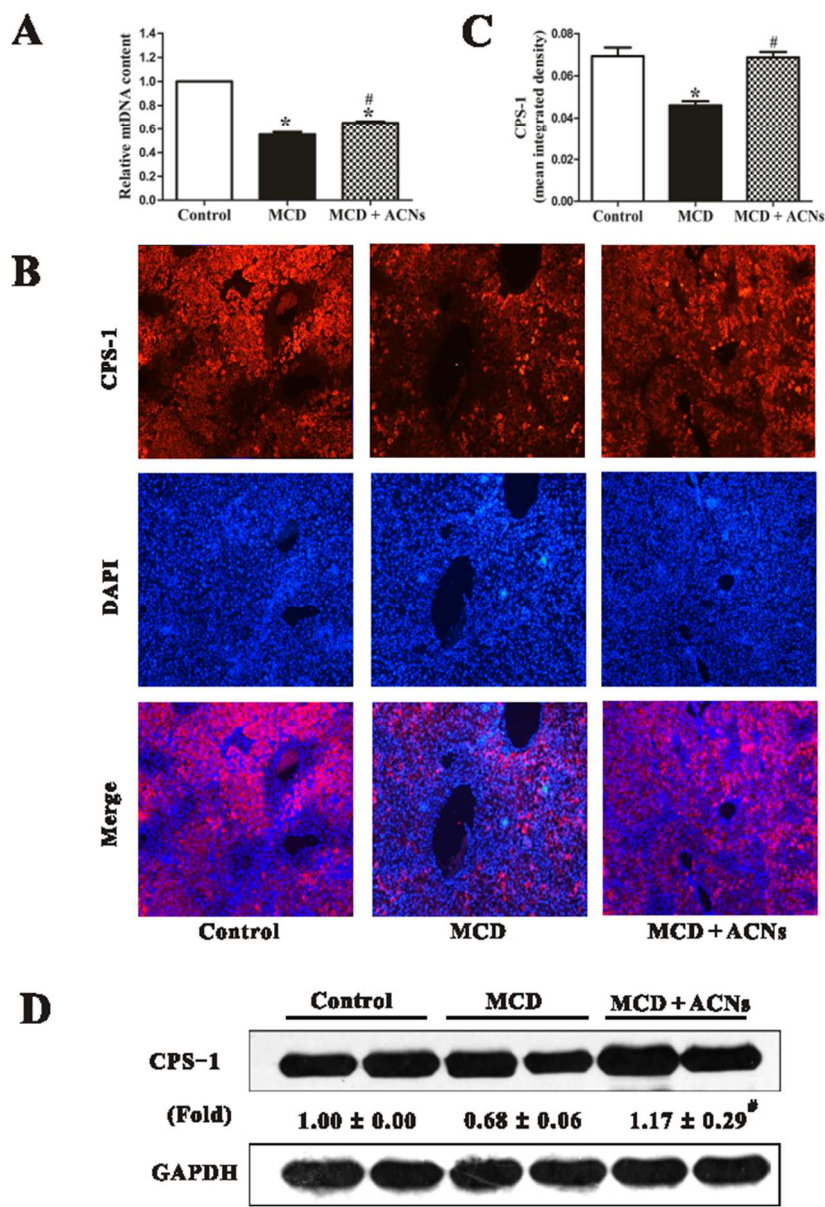


Figure 5. ACNs attenuated reduction of mitochondrial content and function in NASH. (A) Mitochondrial genome copy number was shown as the ratio of mtDNA to nDNA from purified liver DNA, which was determined by quantitative real-time PCR. The control group was set to be 1. (B) Representative immunofluorescent photomicrographs (200 × magnification) for mitochondrial marker CPS-1 (red fluorescence) showed granular staining patterns in liver frozen sections. (C) Fluorescent staining of CPS-1 per field was quantified by Image J software and reported as mean integrated density. (D) Western blot analysis was performed to semi-quantitatively assess expression levels of CPS-1 from liver homogenates. The control group was set to be 1. Values are expressed as mean ± SD, n = 8. \*P < 0.05 versus the control group; #P < 0.05 versus the MCD group.  
56x79mm (300 x 300 DPI)

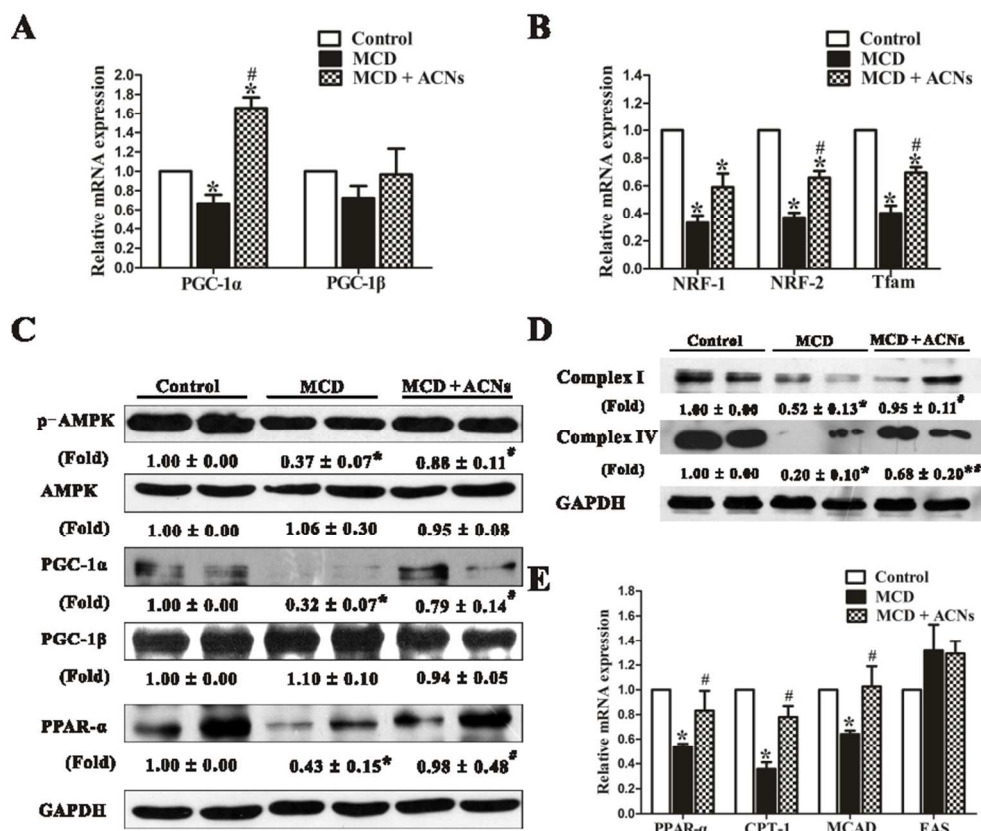
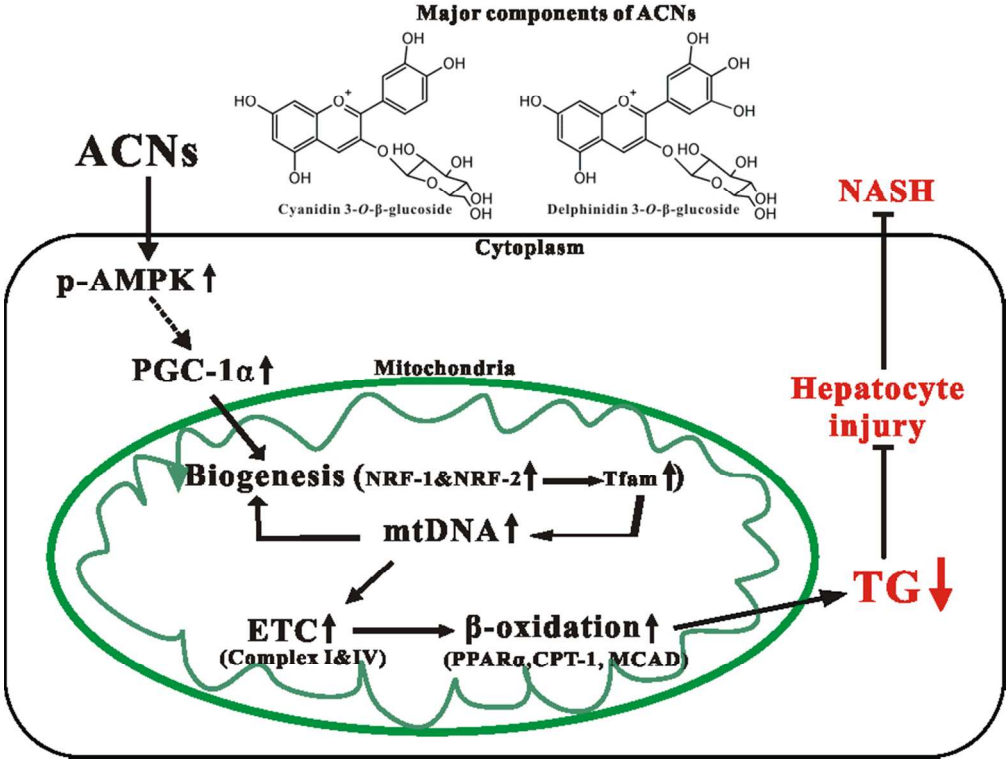


Figure 6. ACNs stimulated mitochondrial biogenesis and improved mitochondrial ETC defects as well as enhanced mitochondrial  $\beta$ -oxidation in NASH. (A-B) Real-time PCR was applied to measure mRNA expression of PGC-1 $\alpha$  and PGC-1 $\beta$  (A) and genes related to mitochondrial biogenesis (NRF-1, NRF-2 and Tfam) (B). (C) Protein expression of p-AMPK, total AMPK, PGC-1 $\alpha$ , PGC-1 $\beta$  and PPAR- $\alpha$  in livers were measured by Western blot, quantified using densitometry and normalized by GAPDH content. (D) Protein levels of Complex I and IV were examined by Western blot. (E) Genes related to fatty acid oxidation (CPT-1, MCAD and PPAR- $\alpha$ ) and lipogenesis (FAS) were subjected to RT-PCR analysis. The control group was set to be 1. Results are expressed as mean  $\pm$  SD, n = 6-8. \*P < 0.05 versus the control group; #P < 0.05 versus the MCD group. 79x67mm (300 x 300 DPI)



Graphic abstract  
79x60mm (300 x 300 DPI)